Biochemical and Biophysical Research Communications 391 (2010) 159–165

Contents lists available at ScienceDirect

Biochemical and Biophysical Research Communications

journal homepage: www.elsevier.com/locate/ybbrc

Functional and structural characterization of the talin F0F1 domain

Prerna N. Domadia [1], Yan-Feng Li [1], Anirban Bhunia, Harini Mohanram, Suet-Mien Tan [*], Surajit Bhattacharjya [*]

School of Biological Sciences, Nanyang Technological University, 60 Nanyang Drive, Singapore 637551, Singapore

ARTICLE INFO

Article history:
Received 15 October 2009
Available online 10 November 2009

Keywords:
Integrin
Talin
Cell adhesion
NMR
LFA-1
Folding

ABSTRACT

The globular head domain of talin, a large multi-domain cytoplasmic protein, is required for inside-out activation of the integrins, a family of heterodimeric transmembrane cell adhesion molecules. Talin head contains a FERM domain that is composed of F1, F2, and F3 subdomains. A F0 subdomain is located N-terminus to F1. The F3 contains a canonical phosphotyrosine binding (PTB) fold that directly interacts with the membrane proximal NPxY/F motif in the integrin β cytoplasmic tail. This interaction is stabilized by the F2 that interacts with the lipid head-groups of the plasma membrane. In comparison to F2 and F3, the properties of the F0F1 remains poorly characterized. Here, we showed that F0F1 is essential for talin-induced activation of integrin αLβ2 (LFA-1). F0F1 has a high content of β-sheet secondary structure, and it tends to homodimerize that may provide stability against proteolysis and chaotrope induced unfolding.

Introduction

Cell–cell and cell–extracellular matrix (ECM) adhesion are essential for the development and homeostasis of metazoans. An increasing number of cytoplasmic proteins are reported to assemble at the focal adhesion sites, and many of these are required for the induction and strengthening of these sites [1]. Talin (~270 KDa), an adaptor protein, is well known to induce cell adhesion by binding to the integrin β cytoplasmic tails that leads to the separation of the integrin α and β subunits with its concomitant activation [2–5]. In vertebrates, two talin genes, talin 1 and talin 2 have been reported [6,7]. Talin consists of multiple domains having distinct functions [5]. The N-terminal head region (residues 1–400) is composed of the FERM domain containing F1, F2, and F3 domains with a further extension towards N-terminus termed as F0 domain. On the other hand, the C-terminal of talin (residues 482–2541) defines a long helical rod region with multiple bundles of α-helices [5]. The helical rod region is primarily involved in binding to cytoskeletal proteins F-actin and vinculin [5], and it is also involved in maintaining an inactivated talin [8]. The head region of talin functions as an activator of integrins by binding directly to the cytoplasmic region of the β tails [2,4]. Structural study reveals that talin F3 contains a phosphotyrosine binding (PTB) fold that interacts with the membrane proximal NPxY motif of the β3 cytoplasmic tail [9]. The disruption of a membrane proximal salt-bridge in the integrin cytoplasmic tails triggers integrin activation [10,11]. Recent structural study reveals that the conserved K327 in talin 2 (K324 in talin 1) interacts with D759, which is involved in salt-bridge formation, in the integrin β1D cytoplasmic tail [4]. This interaction disrupts the integrin cytoplasmic tails salt-bridge. Because talin interaction with integrin cytoplasmic tail is weak in a cell-free system, it was proposed that a basic patch in the talin F2 interacts with the phosphatidyl head-groups of the inner plasma membrane leaflet to stabilize the talin-integrin association [4].

The talin F2 and F3 domains are important for the activation of integrins, but the F0 and F1 domains are also required for the activation of integrins α5β1 and αIIbβ3 despite differences in the level of activation [12]. In this report, we showed that the F0F1 is required for talin-induced activation of the leukocyte integrin LFA-1. Biophysical, NMR, and CD structural studies reveal that talin F0F1 is well folded with a high content of β-sheet structures. The F0F1 appears to exist as a dimer in solution and it exhibits a two step cooperative urea-induced unfolding process. These functional, structural and stability characterization data suggest that talin F0F1 has an important role in the function of talin.

Materials and methods

cDNA expression plasmids. The full-length αL and β2 cDNA in pcDNA3.0 expression plasmids have been reported previously [13]. The human talin 1 head domain (M1-Q435) cDNA in expression plasmid pXJ40-HA was reported previously [11], and it was used as the template for the generation of HA-tagged talin F0F1 (M1-D205) and F2F3 (S206–S405) in pXJ40-HA using standard

* Corresponding authors. Fax: +65 6791 3856.
E-mail addresses: smtan@ntu.edu.sg (S.-M. Tan), surajit@ntu.edu.sg (S. Bhattacharjya).
[1] These authors contributed equally to this study.

0006-291X/$ - see front matter © 2009 Elsevier Inc. All rights reserved.
doi:10.1016/j.bbrc.2009.11.024

molecular biology procedures. All constructs were verified by DNA sequencing (First Base, Singapore).

Cell culture, transfection, and flow cytometry analyses. 293T cells were obtained from ATCC (Manassas, VA) and were cultured in complete RPMI medium containing 10% (v/v) heat-inactivated fetal bovine serum (FBS) and 100 IU/mL penicillin, and 100 μg/mL streptomycin (JRH Biosciences Inc.). Cells were transfected with αL, β2, and talin expression plasmids (2 μg each) using the Polyfect transfection reagent (Qiagen). Cell surface expression of αLβ2 was determined by flow cytometry analyses (FACS-Calibur, BD Bioscience) using the mAb MHM24 (αL-specific, kindly provided by A. McMichael, John Radcliffe Hospital, Oxford, UK) as described previously [13].

Cell adhesion assay on immobilized ICAM-1. The adhesive properties of 293T transfectants onto immobilized αLβ2-ligand ICAM-1 were determined using exactly the method as described previously [14]. Mg/EGTA (5 mM $MgCl_2$ and 1.5 mM EGTA) was included to promote activation of αLβ2. To demonstrate specific αLβ2-mediated adhesion onto ICAM-1, the function-blocking mAb MHM24 (10 μg/ml) was also included.

Western blotting and immunoprecipitation. To detect the expressions of different talin constructs, transfectants were lysed in lysis buffer containing 10 mM Tris–HCl, pH 8.0, 150 mM NaCl, 1% (v/v) NP-40, and protease inhibitors cocktail (Roche). Proteins were resolved on a 7.5% SDS–PAGE under reducing conditions. HA-talin constructs expressions were examined by immunoblotting with rabbit anti-HA antibody (Delta Biolabs), HRP-conjugated donkey anti-rabbit IgG followed by enhanced chemiluminescence (ECL) detection (both from Amersham Biosciences). To assess the conformation of the αLβ2 in 293T cells co-transfected with different talin constructs, cells were incubated in complete medium containing 10 μg/ml of mAb KIM127 (reporter antibody that binds to fully extended β2 integrins) [15,16] at 37 °C for 30 min. Thereafter, cells were washed in medium to remove unbound antibody and lysed in lysis buffer. The αLβ2-KIM127 complex was precipitated with protein A Sepharose beads (Amersham Biosciences). Proteins were resolved on a 7.5% SDS–PAGE under reducing conditions, and the αL protein band was examined using an αL-specific mAb (clone 27, BD transduction lab), HRP-conjugated sheep anti-mouse IgG (Amersham Biosciences), followed by ECL detection.

F0F1 cloning, expression and purification. The F0F1 domain (M1-D205) of talin head was over-expressed as a recombinant F0F1 fusion protein containing a non-cleavable C-terminal His6-tag. *Escherichia coli* BL21 (DE3) cells containing cloned F0F1 gene in a pET13 vector were growing at 37 °C in presence of 30 μg/ml kanamycin; either in a rich LB medium or in a M9 medium supplemented with ^{15}N ammonium chloride (Cambridge Isotope Lab.) and ^{12}C-glucose. The cells were induced at an OD_{600} of 0.8 with 1 mM IPTG. After incubating for 9–12 h at 18 °C for protein expression, cells were harvested, resuspended in 20 mM Tris–hydrochloride buffer, pH 8.0, and further lysed by sonication. The clarified supernatant was applied onto Ni–NTA column for His-tag affinity purification (Qiagen) and protein was eluted with 500 mM imidazole. Further, size exclusion chromatography was carried out using FPLC in a superdex G75 column to obtain pure protein samples.

Limited proteolysis experiment. Purified native F0F1 at 40 μM was incubated with bovine pancreas α-chymotrypsin (Sigma), at each of two protein–protease molar ratios of 50:1 and 1000:1, at 30 °C. The proteolysis buffer consisted of 10 mM sodium phosphate, 50 mM NaCl and 10 mM β-marcaptoethanol (β-ME) at pH 7.3. The proteolytic digestion was stopped at variable time points ranging from 15 min to 13 h by addition of 10× protease inhibitor mix (Roche). Proteolytic reactions were finally analyzed by SDS–PAGE electrophoresis and visualized using Coomassie Brilliant Blue dye.

NMR experiments. All NMR experiments were performed at 25 °C on a Bruker DRX 600 MHz NMR spectrometer, equipped with an actively shielded cryoprobe and pulse field gradient. $^{1}H–^{15}N$ HSQC spectra of F0F1 were recorded using a ^{15}N labeled sample at 0.5 mM concentration in 10 mM sodium phosphate buffer, pH 5.8, containing 20 mM NaCl, and 2 mM Tris-(2-carboxyethyl)-phosphine hydrochloride (TCEP). The three-dimensional $^{1}H–^{15}N$ HSQC–NOESY experiments were performed at a mixing time of 200 ms. NMR data were processed using the Topspin program suite (Bruker) and analyzed by Sparky (T.D. Goddard and D.G. Kneller, University of California, San Francisco). The hydrodynamic radius of F0F1 was calculated using pulse field gradient (PFG) NMR method with PG-SLED pulse sequence as described earlier [17,18]. The gradient strength was incremented from 2% to 95% using a series of one-dimensional ^{1}H NMR experiments. The decay of the ^{1}H resonance signals were then fitted to a single Gaussian expression: $I(g) = Ae^{-dg^2}$, where I, g, and d represent intensity of the signals, gradient strengths and decay rates, respectively. The hydrodynamic radii were calculated using the equation $R_h^{pro} = (d_{ref}/d_{pro}) \times R_h^{ref}$ (17, 18) where, R_h^{pro} is the hydrodynamic radius of F0F1 and d_{ref} and d_{pro} are the decay rate of reference molecule, CH_3COO^- and protein, respectively. Sodium acetate was used as a reference molecule.

CD spectroscopy. Far- and near-UV CD spectra of F0F1 domain were recorded using a Chirascan Circular Dichroism spectropolarimeter (Applied Photophysics Ltd., UK) in 10 mM sodium phosphate at pH 7.0, at 20 °C, in the absence and presence of denaturant 8 M urea. The far-UV spectra of 20 μM of F0F1 were scanned at the wavelength range of 190–240 nm, in a 0.01 cm path length cuvette, using a bandwidth of 0.5 nm and averaging over three scans. Likewise, near-UV spectra of 100 μM F0F1 were scanned at the wavelength range of 250–320 nm, in a 1 cm path length cuvette, using a bandwidth of 0.2 nm, and averaging for three scans. Respective baseline scans were obtained using the same acquisition parameters for the native buffer alone and in presence of 8 M urea; which were further subtracted from the respective data scans of F0F1. The corrected data obtained in millidegree (θ) were converted to molar ellipticity in deg cm^2 $dmol^{-1}$.

Fluorescence measurements. The intrinsic tryptophan fluorescence spectra of F0F1 were recorded on a Cary Eclipse fluorescence spectrophotometer (Varian, Inc.). All measurements were made using sample concentration 5 μM of F0F1 in a 0.1 cm path length quartz cuvette at 20 °C. The band passes for excitation (295 nm) and emission were set to 2.5 nm and emission were scanned in wavelength region between 300–400 nm. Unfolding studies for native F0F1 was performed by titrating increasing concentrations of urea, ranging from 0.2 to 8.0 M, in a buffer containing 10 mM sodium phosphate, 50 mM sodium chloride, and 10 mM β-ME, pH 7.0. Fluorescence quenching studies by acrylamide were performed for native F0F1, and for its denatured state in 8 M Urea. Aliquots from 5 M acrylamide stock solution were added to 5 μM of F0F1 in the native buffer at 20 °C. Fluorescence emission at 343 nm, showing maximum intensity, was monitored for quenching. Stern–Volmer plot for acrylamide quenching of fluorescence of F0F1; in its native and denatured states were plotted, where F0 and F were the fluorescence intensities in the absence and presence of the quencher.

Results and discussion

Requirement of talin 1 F0F1 in integrin αLβ2 activation

Herein, we made use of human talin 1 (henceforth referred to as talin) to address the requirement of F0F1 domains in talin activation of integrin LFA-1. Previously, we reported that talin head (M1-Q435) activates integrin LFA-1 [11]. Here, we generated two additional constructs F0F1 (M1-D205) and F2F3 (S206–S405) (Fig. 1A). All constructs contain an N-terminal HA-tag. 293T cells were transfected with talin head, F0F1, or F2F3 with full-length αL and β2 expression plasmids. The expression of LFA-1 was

comparable in all transfectants as determined by flow cytometry analyses using mAb MHM24 (αL-specific), and the expression of the different talin constructs verified by anti-HA immunoblotting (Fig. 1B). Cell adhesion assay on immobilized ICAM-1 was performed with these transfectants with or without the addition of the LFA-1 activating agents Mg/EGTA (Fig. 1C). In the absence of Mg/EGTA, only talin head-expressing transfectants showed significant adhesion to ICAM-1. In the presence of Mg/EGTA, all transfectants adhered to ICAM-1. The adhesion was specific to LFA-1 because inclusion of the αL-specific function-blocking mAb MHM24 abrogated all adhesion events. Next, we examined the conformation of LFA-1 in transfectants expressing these talin constructs. We use the conformational reporter mAb KIM127 that binds to a highly extended β2 integrin to detect activated LFA-1 by the method of immunoprecipitation with KIM127 followed by immunoblotting the integrin αL subunit (Fig. 1D) [15,16]. High level of αL signal was detected in cells transfected with talin head but not F0F1 or F2F3. Together, these data suggest that F0F1 is required for the activating function of talin head on integrin LFA-1. These data are in line with the requirement of F0F1 in talin activation of integrins as reported for integrins α5β1 and αIIbβ3 [12].

Oligomerization and folding of talin F0F1

Fig. 2A shows $^{1}H–^{15}N$ HSQC spectrum of F0F1 domain of talin. A large dispersion of amide protons (6.5–9.5 ppm) and ^{15}N resonances demonstrates that the F0F1 is an independently folded domain of talin (Fig. 2A). There was a number of upfield shifted (0.5 to −0.2 ppm) resonances in the one-dimensional proton NMR spectra of F0F1 (Fig. 2A, inset). These NMR resonances are characteristic of an intimate packing among the aromatic rings with the aliphatic sidechains in the well folded proteins [19]. The three-dimensional ^{15}N-edited HSQC–NOESY spectra revealed a number of NOE connectivity among amide protons with the upfield shifted methyl resonances, indicating a well packed structure of F0F1 (Supplementary Fig. 1). The line-width of $^{1}H–^{15}N$ HSQC cross-peaks appeared to be rather broadened, suggesting that F0F1 domain may not exist as a monomeric species in solution (Fig. 2A). The oligomerization of F0F1 domain was further investigated by NMR pulse field gradient and size exclusion chromatography methods. Fig. 2B shows a plot of hydrodynamic radii (R_H) of a number of proteins vs number of amino acid residues. Clearly, the $R_H \sim 26$ Å of F0F1 measured from NMR-PFG is significantly higher than expected for a 200-residue protein (Fig. 2B), indicating a plausible dimerization of F0F1 domain. The measurement of molecular weight of F0F1 using size exclusion chromatography also indicated that a F0F1 domain of talin dimerizes in solution (Fig. 2C).

Secondary structure and stability of talin F0F1

Fig. 3 summarizes secondary structure and unfolding/stability of the F0F1 domain determined by CD and fluorescence spectroscopy. The far-UV CD spectra, determining secondary structure content, of F0F1 demonstrate a negative band around 208–210 nm wavelength with another negative CD band around 218–220 nm (Fig. 3A). The far-UV CD spectra of F0F1 do not represent a highly or all helical protein with a more intense CD band at 222 nm and a less or equal intense CD band at 208 nm. The CD spectra of F0F1 also do not indicate an all β-sheet protein with a diagnostic negative CD band at 218 nm. Therefore, the CD spectra of F0F1 may indicate mixed secondary structures consisted of α-helical and β-sheet structures. A deconvolution of the CD spectra, using K2D2 program [20], of F0F1 domain of talin yielded 27% of β-sheet and 18% of helical secondary structures. The F0F1 domain contains as many as 5 Phe (F19, F47, F50, F198, and F199), 6 Tyr (Y26, Y70, Y71, Y81, Y127, and Y199) and 2 Trp (W61 and W173) residues. These aromatic residues are found to be distributed through out the primary amino acid sequence (residues M1-D205) of F0F1 pro-

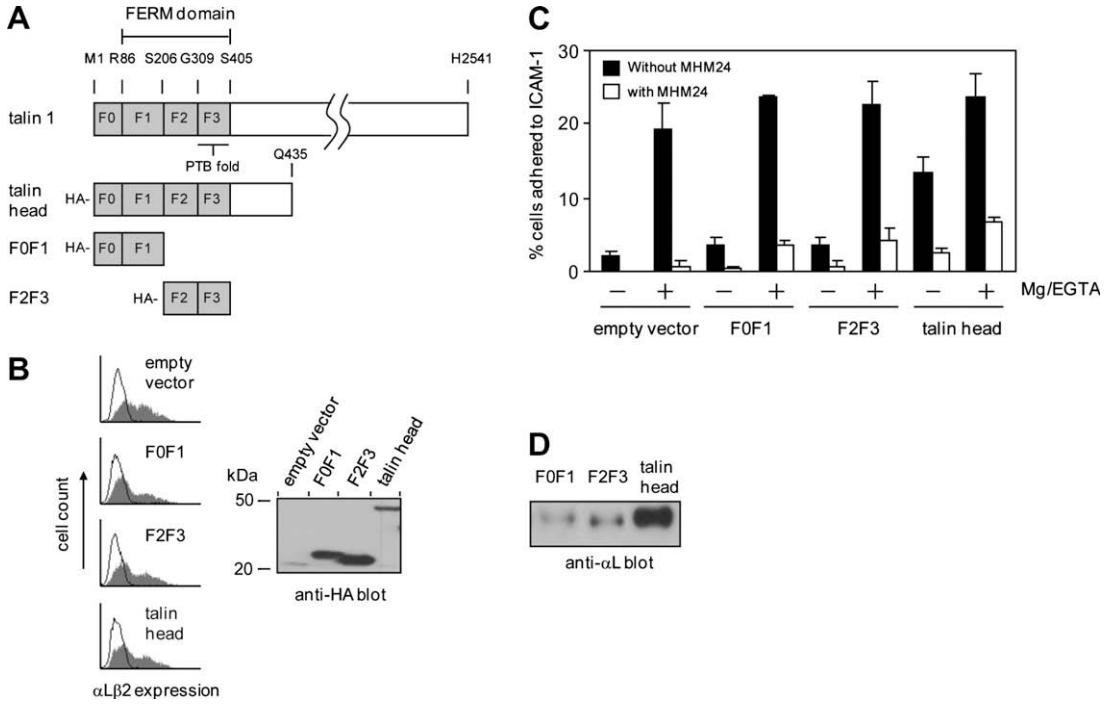

Fig. 1. F0F1 domain is required for talin-induced integrin LFA-1 activation. (A) Illustration of the different talin constructs used in this study. (B) Flow cytometry analyses of integrin LFA-1 expression on 293T transfectants co-transfected with different talin constructs. mAb MHM24 (integrin αL-specific) was used as the primary antibody (shaded histogram). Irrelevant control IgG (open histogram). Western blot to detect expressions of talin constructs in transfectants using anti-HA antibody. (C) Adhesion of cells transfected with LFA-1 and different talin constructs to immobilized ICAM-1. The function-blocking mAb MHM24 was included to demonstrate LFA-1-mediated adhesion specificity. (D) Immunoprecipitation analyses of the conformation of LFA-1 in 293T transfectants expressing different talin constructs using the conformational reporter mAb KIM127. Immunoprecipitated αL protein band was detected by immunoblotting with anti-αL antibody as described in Materials and methods.

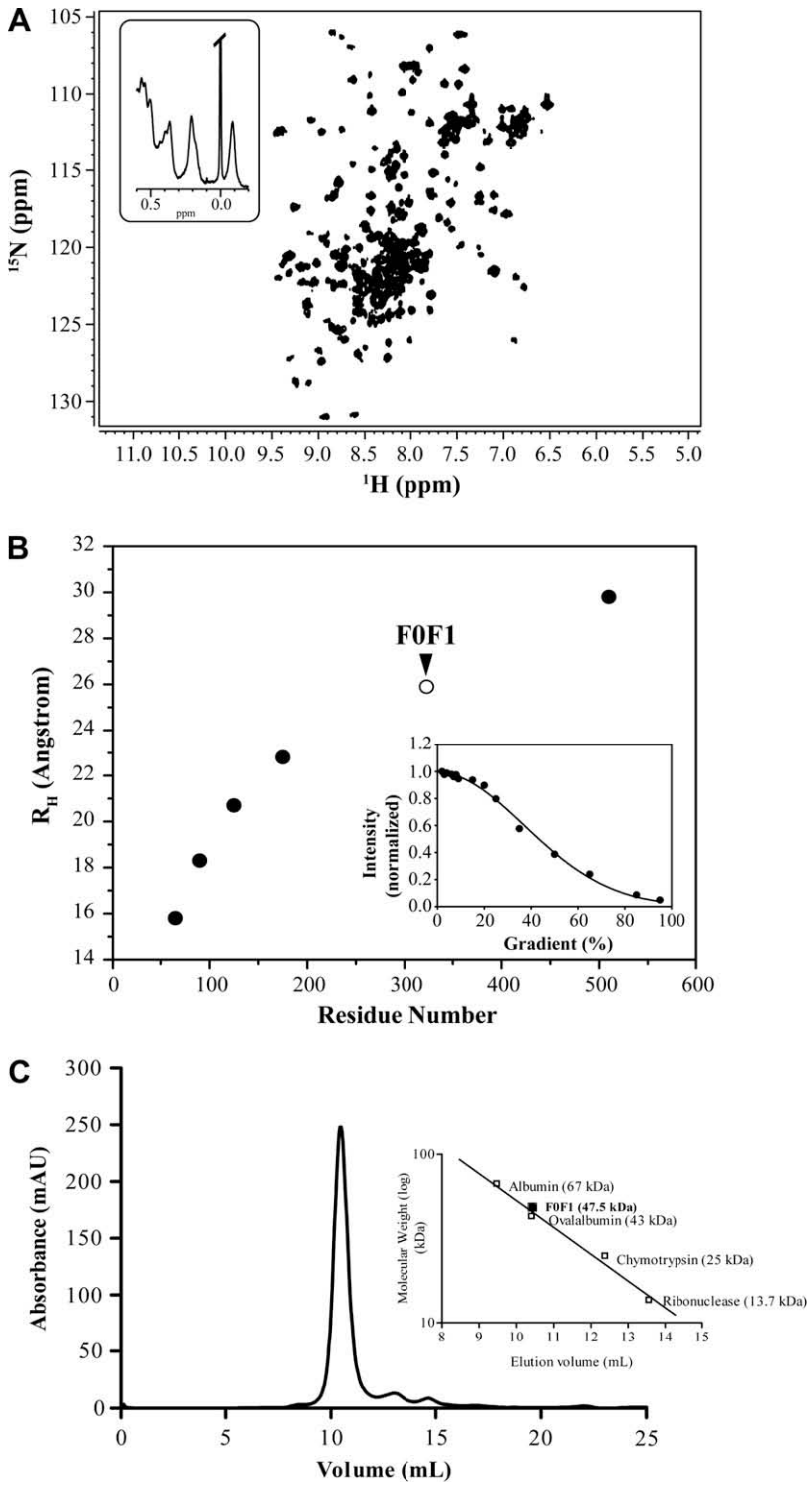

Fig. 2. Folding and dimerization of F0F1 domain of talin. (A) ^{1}H–^{15}N heteronuclear single quantum coherence (HSQC) spectrum of F0F1. (inset) One-dimensional ^{1}H NMR spectrum showing the upfield shifted resonances. (B) Plot showing hydrodynamic radii of F0F1 and some reference proteins of various molecular weight [18]. (inset) Normalized intensity of the upfield shifted resonance (–0.2 ppm) of F0F1 as a function of gradient strength. (C) FPLC chromatographic trace of F0F1 at 276 nm as a function of retention volume in 10 mM sodium phosphate buffer, pH 7.2, containing 50 mM NaCl and 10 mM β-ME.

viding an excellent probe to assess global structure and stability of the domain. The near-UV CD spectra of F0F1 demonstrate intense positive bands at 260–280 nm and also at 290 nm (Fig. 3B). The near-UV CD bands at 260–280 nm can be attributed to the Phe and Tyr residues, whereas CD signals at 290 nm are arising from absorbance of Trp residues. The near-UV CD spectra of F0F1 are therefore indicating asymmetric environments of the aromatic chromophore as a result of a well packed hydrophobic core. The fluorescence emission maximum of Trp residue is highly sensitive to the environment [21]. The emission maxima of Trp of F0F1 domain are remarkably blue shifted to 343 nm, demonstrating that the two Trp residues (W61 and W173) are buried inside the hydrophobic core of the protein (Fig. 3C). The diminution of the Trp fluorescence intensity by addition of exogenous quenchers indicates

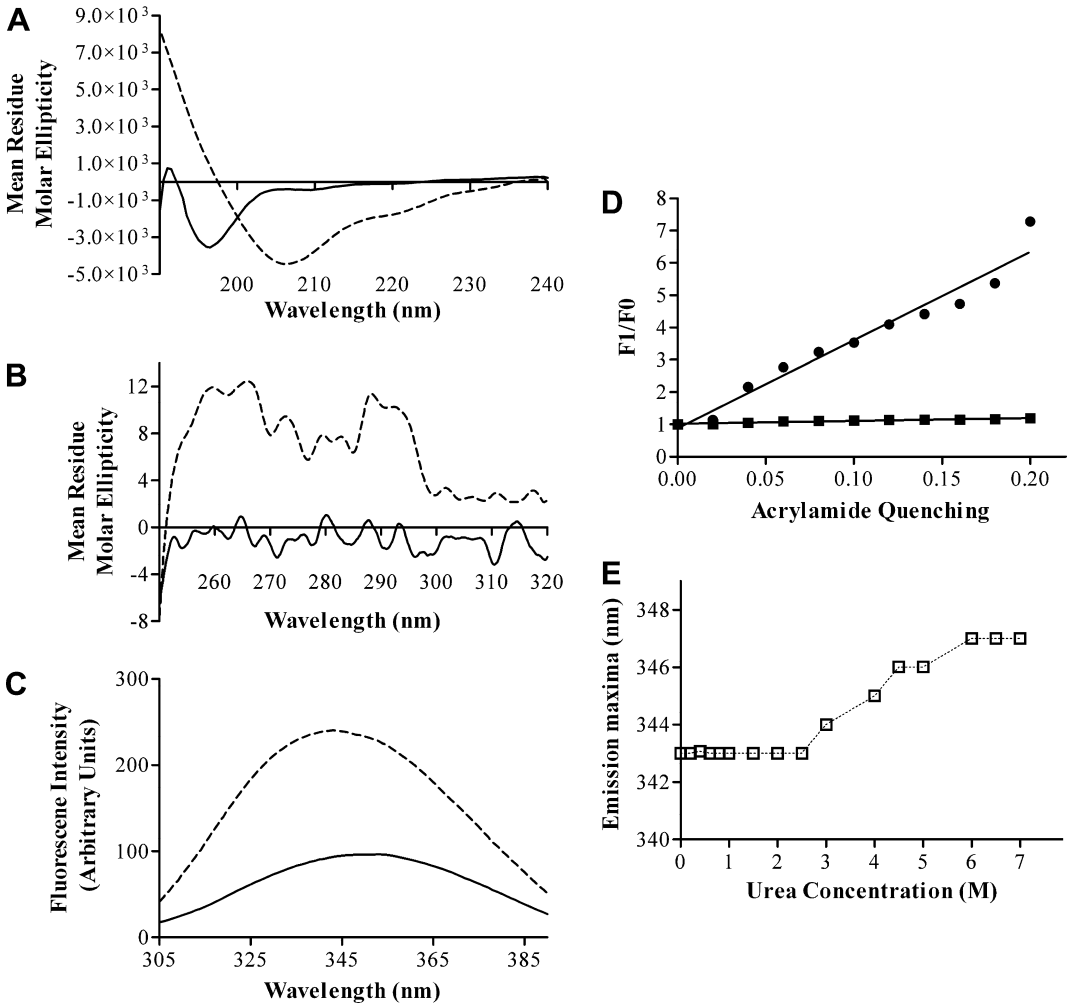

Fig. 3. Secondary structure and stability of F0F1 domain of talin. (A) The far-UV CD (B) the near-UV CD and (C) intrinsic tryptophan fluorescence emission spectra of F0F1 domain in the native and in the presence of 8 M urea are shown as dashed and solid lines, respectively. (D) The modified Stern–Volmer plot of fluorescence quenching of F0F1 in the native state (solid squares) and in 8 M Urea (solid circles). (E) Plot showing changes of the fluorescence emission maxima of tryptophan residues of F0F1 domain of talin as a function of concentrations of urea.

extent of exposure of Trp residues to the aqueous solution [21]. Fluorescence quenching experiments for F0F1 were carried out by non-ionic water soluble quencher acrylamide. The Stern–Volmer quenching plot shows that Trp residues of F0F1 experience only a limited quenching (Fig. 3D), indicating both Trp are protected against quenching effect. Taken together, these data demonstrate that the functional F0F1 domain of talin is globally folded with a high content of β-sheet secondary structures.

Urea-induced unfolding was carried out to determine the stability and cooperativity of the F0F1 domain structure. The F0F1 domain is found to be largely unfolded at high concentration of denaturant 8 M urea. The far-UV CD spectra of F0F1 obtained in presence of 8 M urea shows a single negative CD band at 195 nm characteristic of random conformations (Fig. 3A), followed by a dramatic decrease in the intensity of the near-UV CD bands at this urea concentration (Fig. 3B). These data suggest that at 8 M urea both the native secondary and tertiary packing of the F0F1 domain are largely abolished. The intrinsic Trp fluorescence experiments show a red shifted emission maxima ~352 nm for Trp residues at 8 M urea (Fig. 3C), with a high exposure to the acrylamide quencher compared to the native state (Fig. 3D). Therefore, at 8 M urea both Trp residues of F0F1 are appeared to be solvent exposed implying unfolded conformations. The urea-induced unfolding transition of F0F1was further monitored using change in Trp emission maxima as a function of concentration of urea (Fig. 3E). As can be seen, there was no change in the emission maxima of Trp residues till 3 M urea concentration, indicating protein retains its native state conformation at this urea concentration. However, a further increase of denaturant concentration had caused a dramatic change in the emission maxima of Trp, towards the longer wavelength (or red shift), indicating unfolding of the F0F1 domain (Fig. 3E). The transition appeared to be complete only at a urea concentration of 6 M (Fig. 3E). There was no significant change in the emission maxima above 6 M concentration of denaturant (Fig. 3E). These results suggest that F0F1 domain of talin undergoes a cooperative two state unfolding transition in urea with a midpoint of unfolding occurring at 4.5 M urea concentration (Fig. 3E). We have examined stability of the F0F1 domain against proteolysis by protease chymotrypsin (Fig. 4). The well folded domain appears to be resistant against proteolysis. A complete digestion by chymotrypsin of the F0F1 domain should yield 49 potential peptide fragments. At a protein:protease ratio of 1000:1, there was no significant cleavage detected even upon incubation to 13 h (Fig. 4B), as judged by the persistent intensity of F0F1 protein band, around 23 Kda, in SDS–PAGE gel. At a higher concentration of protease at a ratio of F0F1: protease 50:1 a limited proteolysis can be seen (Fig. 4B), indicating protease accessibility of a certain region of the domain at higher chymotrypsin concentrations.

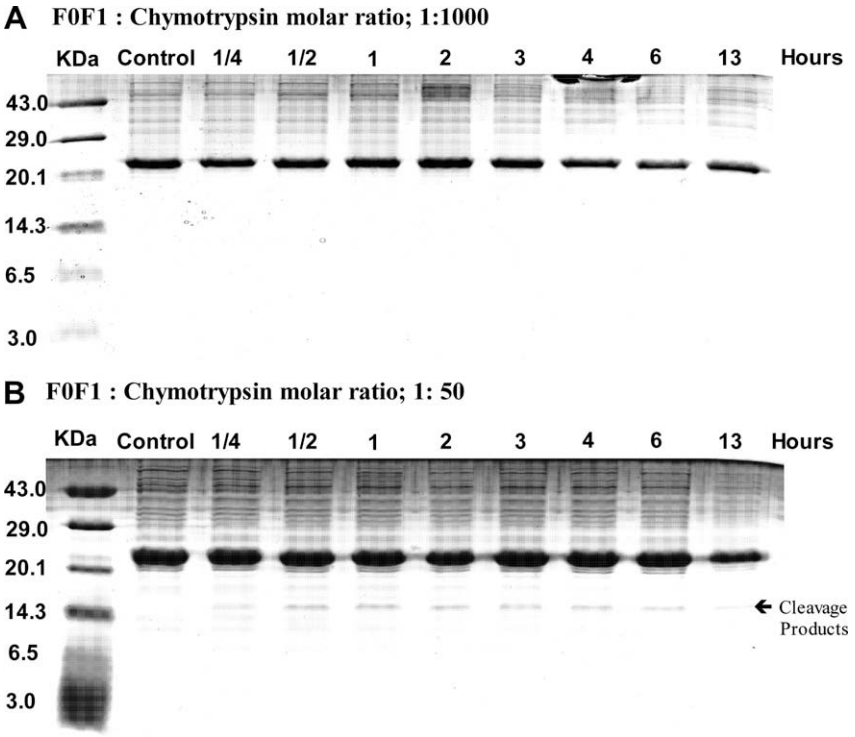

Fig. 4. Proteolytic digestion of F0F1 domain of talin. SDS–PAGE gel electrophoresis analysis of F0F1 upon incubation with protease chymotrypsin as a function of time at a molar ratio of protease: protein (A) 1:1000 and (B) 1:50. The molecular weights of the standard protein marker are shown on the left followed by a control (no chymotrypsin) and in presence of chymotrypsin.

Conclusions

A large body of evidence points to the importance of cytoplasmic proteins interacting with the integrin cytoplasmic tails in the regulation of integrin function [22]. Talin has been the focus of many of these studies because of its well established role as an activator of integrin function, and its function as a linker molecule that connects the integrin to the cytoskeleton [5]. The molecular details of talin-induced integrin activation begin to unfold as more biophysical and structural studies are performed [3,4,23,24]. As compared to the F2 and F3 domains within the talin head region, much less is known of the structure and function of the talin F0F1. Here, we showed that F0F1 is essential for the activation of integrin LFA-1. Recently, the F0 domain of kindlin-1, which belongs to a family of FERM-containing co-activators of integrins, was shown to adopt an ubiquitin-like β-grasp fold, and talin F0 shares a similar fold [8]. It was also shown that kindlin-1 F0 is required for the targeting of kindlin-1 to integrin αIIbβ3 focal adhesion sites [8]. Whether talin F0 serves a similar function remains to be determined. In this study, we also observed an interesting property of talin F0F1 with a propensity to form homodimer having high stability against proteolysis and chaotrope induced unfolding. The F0F1 homodimer undergoes a cooperative two state unfolding at a high urea denaturant concentration. In future studies, we will determine the three-dimensional structure of the talin F0F1 coupled with mutagenesis studies to elucidate the physiological significance of the aforementioned properties.

Acknowledgments

This work was supported by Grants AcRF RG 34/08 M52080103 (S.M.T.) and A∗STAR BMRC 08/01/22/19/556 (S.B. and S.M.T.).

Appendix A. Supplementary data

Supplementary data associated with this article can be found, in the online version, at doi:10.1016/j.bbrc.2009.11.024.

References

[1] S. Liu, D.A. Calderwood, M.H. Ginsberg, Integrin cytoplasmic domain-binding proteins, J. Cell Sci. 113 (Pt. 20) (2000) 3563–3571.
[2] S. Tadokoro, S.J. Shattil, K. Eto, V. Tai, R.C. Liddington, J.M. De Pereda, M.H. Ginsberg, D.A. Calderwood, Talin binding to integrin beta tails: a final common step in integrin activation, Science 302 (2003) 103–106.
[3] M. Kim, C.V. Carman, T.A. Springer, Bidirectional transmembrane signaling by cytoplasmic domain separation in integrins, Science 301 (2003) 1720–1725.
[4] N.J. Anthis, K.L. Wegener, F. Ye, C. Kim, B.T. Goult, E.D. Lowe, I. Vakonakis, N. Bate, D.R. Critchley, M.H. Ginsberg, I.D. Campbell, The structure of an integrin/talin complex reveals the basis of inside-out signal transduction, EMBO J. (2009).
[5] G.C. Roberts, D.R. Critchley, Structural and biophysical properties of the integrin-associated cytoskeletal protein talin, Biophys. Rev. 1 (2009) 61–69.
[6] S.J. Monkley, C.A. Pritchard, D.R. Critchley, Analysis of the mammalian talin2 gene TLN2, Biochem. Biophys. Res. Commun. 286 (2001) 880–885.
[7] M.A. Senetar, R.O. McCann, Gene duplication and functional divergence during evolution of the cytoskeletal linker protein talin, Gene 362 (2005) 141–152.
[8] B.T. Goult, N. Bate, N.J. Anthis, K.L. Wegener, A.R. Gingras, B. Patel, I.L. Barsukov, I.D. Campbell, G.C. Roberts, D.R. Critchley, The structure of an interdomain complex that regulates talin activity, J. Biol. Chem. 284 (2009) 15097–15106.
[9] B. Garcia-Alvarez, J.M. de Pereda, D.A. Calderwood, T.S. Ulmer, D. Critchley, I.D. Campbell, M.H. Ginsberg, R.C. Liddington, Structural determinants of integrin recognition by talin, Mol. Cell 11 (2003) 49–58.
[10] P.E. Hughes, F. Diaz-Gonzalez, L. Leong, C. Wu, J.A. McDonald, S.J. Shattil, M.H. Ginsberg, Breaking the integrin hinge. A defined structural constraint regulates integrin signaling, J. Biol. Chem. 271 (1996) 6571–6574.
[11] Y.F. Li, R.H. Tang, K.J. Puan, S.K. Law, S.M. Tan, The cytosolic protein talin induces an intermediate affinity integrin aLb2, J. Biol. Chem. 282 (2007) 24310–24319.
[12] M. Bouaouina, Y. Lad, D.A. Calderwood, The N-terminal domains of talin cooperate with the phosphotyrosine binding-like domain to activate beta1 and beta3 integrins, J. Biol. Chem. 283 (2008) 6118–6125.
[13] R.H. Tang, E. Tng, S.K. Law, S.M. Tan, Epitope mapping of monoclonal antibody to integrin aLb2 hybrid domain suggests different requirement of affinity

states for intercellular adhesion molecules (ICAM)-1 and ICAM-3 binding, J. Biol. Chem. 280 (2005) 29208–29216.
[14] X.Y. Tang, Y.F. Li, S.M. Tan, Intercellular adhesion molecule-3 binding of integrin aLb2 requires both extension and opening of the integrin headpiece, J. Immunol. 180 (2008) 4793–4804.
[15] P. Stephens, J.T. Romer, M. Spitali, A. Shock, S. Ortlepp, C.G. Figdor, M.K. Robinson, KIM127, an antibody that promotes adhesion, maps to a region of CD18 that includes cysteine-rich repeats, Cell Adhes. Commun. 3 (1995) 375–384.
[16] N. Beglova, S.C. Blacklow, J. Takagi, T.A. Springer, Cysteine-rich module structure reveals a fulcrum for integrin rearrangement upon activation, Nat. Struct. Biol. 9 (2002) 282–287.
[17] S. Bhattacharjya, P. Xu, H. Xiang, M. Chretien, F. Ni, PH-induced conformational transition of a molten globule like state of the inhibitory prodomain of furin: implications for zymogen activation, Protein Sci. 10 (2001) 934–942.
[18] S. Bhattacharjya, P. Xu, R. Gingras, R. Shaykhutdinov, C. Wu, M. Whiteway, F. Ni, Solution structure of the dimeric SAM domain of MAPKKK Ste11 and its interactions with the adaptor protein Ste50 from the budding yeast: implications in Ste 11 activation and signal transmission through Ste11/Ste50 complex, J. Mol. Biol. 344 (2004) 1071–1087.
[19] K. Wuthrich, NMR of Proteins and Nucleic Acids, John Wiley & Sons Inc., NY, 1986.
[20] C. Perez-Iratxeta, M. Andrade-Navarro, K2D2: estimation of protein secondary structure from circular dichroism spectra, BMC Struct. Biol. 8 (2008) 25.
[21] J.R. Lakowicz, Principles of Fluorescence Spectroscopy, third ed., Springer, New York, 2006.
[22] D.A. Calderwood, J. Cell Sci. 117 (2004) 657–666.
[23] K.L. Wegener, A.W. Partridge, J. Han, A.R. Pickford, R.C. Liddington, M.H. Ginsberg, I.D. Campbell, Structural basis of integrin activation by talin, Cell 128 (2007) 171–182.
[24] A. Bhunia, X.-Y. Tang, H. Mohanram, S.M. Tan, S. Bhattacharjya, NMR solution conformations and interactions of integrin aLb2 cytoplasmic tails, J. Biol. Chem. 284 (2009) 3873–3884.